Topology Simplification of Symmetric, Second-Order 2D Tensor Fields

Xavier Tricoche and Gerik Scheuermann

Computer Science Department, University of Kaiserlautern, P.O. Box 3049, D-67653 Kaiserslautern, Germany, {*tricoche, scheuer*}*@informatik.uni-kl.de*

Summary. Numerical simulations of tubulent flows produce both vector and tensor fields that exhibit complex structural behavior. The topological study of these datasets dramatically reduces the amount of information required for analysis. However, the presence of many features of small scale creates a cluttered depiction that confuses interpretation. In this paper, we extend previous work dealing with vector fields to symmetric, second-order tensor fields. A simplification method is presented that removes degenerate points from the topology pairwise, driven by arbitrary criteria measuring their importance in the overall structure. It is based on an important property of piecewise linear tensor fields that we prove in the paper. Grid and interpolation scheme are preserved since the method uses small local changes of the given discrete tensor values to achieve simplification. The resulting topology is clarified significantly though structurally consistent with the original one. The basic idea behind this technique leads back to the theory of bifurcations and suggests and interpretation as a continuous simplification process.

1 Introduction

Tensors are essential mathematical objects involved in the description of a wide range of scientific and technical fields. They are used for instance in fluid flow, fluid mechanics, civil engineering and medical imaging. Consequently, scientists and engineers need methods to extract essential information from very large tensor datasets that are provided by modern numerical simulations. This explains the increasing interest in tensor field visualization during the last decade. The first topology-based visualization of symmetric, second-order, planar tensor fields was presented by Delmarcelle [2]. Basically, one focuses on one of the two eigenvector fields corresponding to the minor or major eigenvalue. This permits the computation of so-called tensor lines that extend the traditional notion of stream line. The foundations of this technique have been laid down by the work of Helman and Hesselink on vector fields [6]. The theoretical background is provided by the qualitative theory of dynamical systems [1] and differential geometry [9]. The visualization results in a graph representation, where the edges are special tensor lines called separatrices and the nodes are singularities (called degenerate points) of the tensor field, i.e. locations where both eigenvalues are equal. This technique proved suitable for tensor fields with simple structure because the extracted topology contains few degenerate points and separatrices, leading to a clear structure description. Nevertheless, turbulent flows provided by Computational Fluid Dynamics (CFD) simulations or

experimental measurements create cluttered depictions that are of little help for interpretation. Indeed, the topology of such flows is characterized by the presence of a large number of features of very small scale that greatly complicate the global picture of the data. This shortcoming induces a need for simplification methods that prune insignificant features, driven by qualitative and quantitative criteria specific to the considered application. Several techniques have been presented in the past for the simplification of vector fields [5, 8]. The issue of vector field topology simplification was first addressed by de Leeuw and van Liere [7] who proposed a method to prune critical points from the topological graph. However, their approach provides no vector field consistent with the topology after simplification. In previous work [10, 11], we presented a scheme that merges close singular points, resulting in a higher-order singularity that synthesizes the structural impact of several features of small scale in the large. This reduces the number of singularities along with the global complexity of the graph. Nevertheless, this technique has several limitations. First, it implies local grid deformations to simulate the singularities' merging, combined with local modifications of the interpolation scheme. Second, it is unable to remove singularities completely from a given region since a higher-order singularity is always introduced afterward. This is a problem if the goal is to filter out insignificant local features in a given region. Finally, the simplification can only be driven by geometric criteria (the relative distance of neighboring singularities) which prevents to take any additional qualitative aspect into account. The present method extends previous work on vector fields [12] and has been designed to overcome these drawbacks. The basic principle consists in successively removing pairs of degenerate points while preserving the consistency of the field structure. Each of these removals can be interpreted as a forced local deformation that brings a part of the topology to a simpler, equivalent structure. The mathematical background is provided by the theory of bifurcations, originally developed within the qualitative analysis of dynamical systems (see e.g. [4], an application to the tensor case is described in [13]). Practically, the method starts with a planar piecewise linear triangulation. We first compute the topological graph and determine pairs of degenerate points. We retain those that satisfy both a proximity threshold and some relevance criteria specified by the user. The pairs are then sorted with respect to their distance and processed sequentially. For each of them, we determine a cell pad enclosing both degenerate points and slightly modify the tensor values such that both degenerate points disappear. This deformation is controlled by angular constraints on the new eigenvector values while keeping constant those located on the pad boundary. After the processing of all pairs, we redraw the simplified topology.

The paper is structured as follows. We review basic notions of tensor field topology and briefly present the notion of bifurcation in section 2. The special case of piecewise linear tensor fields is considered from the topological viewpoint in section 3. In particular, an angular property of eigenvectors is proven in this context that plays a key role in the following. In section 4, we show how we determine pairs of degenerate points to be removed and sort them in a priority list. Section 5

presents the technique used to locally deform the tensor field in order to remove both singularities of a given pair. Results for a CFD dataset are shown in section 6.

2 Topology of Tensor Fields

The present method deals with a planar triangulation of vertices associated with 2D symmetric second-order tensor values, i.e. symmetric matrices. The interpolation scheme is piecewise linear and provides a matrix valued function defined over the domain. Therefore, we only consider topological features of first order. In this case, topology is defined as the graph built up of all first-order degenerate points and some particular tensor lines connecting them, called separatrices. The required definitions are given next.

2.1 Tensor Lines and Degenerate Points

A real two-dimensional symmetric matrix M has always two (possibly equal) real eigenvalues $\lambda_1 \leq \lambda_2$ with associated orthogonal eigenvectors $\mathbf{e_1}$ and $\mathbf{e_2}$:

$$\forall i \in \{1,2\}, M\mathbf{e_i} = \lambda_i \mathbf{e_i}, \text{with } \mathbf{e_i} \in I\!R^2 \text{ and } \mathbf{e_i} \neq \mathbf{0}.$$

Since the multiplication of an eigenvector by any non-zero scalar yields an additional eigenvector, eigenvectors should be considered without norm nor orientation which distinguishes them fundamentally from classical vectors. Moreover, the computation of the eigenvectors of M is not affected by its isotropic part defined as

$$\frac{1}{\text{tr } M} I_2,$$

where tr M is the trace of M (i.e. the sum of its diagonal coefficients) and I_2 stands for the identity matrix in $I\!R^2 \times I\!R^2$. Consequently, we restrict our considerations to the so-called *deviator* that corresponds to the trace-free part of M. The matrix valued function that we processed is thus of the form:

$$T: (x,y) \in U \subset I\!R^2 \mapsto T(x,y) = \begin{pmatrix} \alpha(x,y) & \beta(x,y) \\ \beta(x,y) & -\alpha(x,y) \end{pmatrix}, \quad (1)$$

where α and β are two scalar functions defined over the considered two-dimensional domain. One defines a major (resp. minor) *eigenvector field* at each position of the domain as the eigenvector related to the major (resp. minor) eigenvalue of the tensor field. For visualization purposes, one restricts the analysis to a single eigenvector field (either minor or major), using the orthogonality of the eigenvectors to extrapolate the topological structure of the other. In an eigenvector field, one defines *tensor lines* as curves everywhere tangent to the eigenvectors. It follows from this definition that these curves have no inherent orientation as opposed to stream lines. Moreover tensor lines cannot be computed at locations where both eigenvalues are equal since

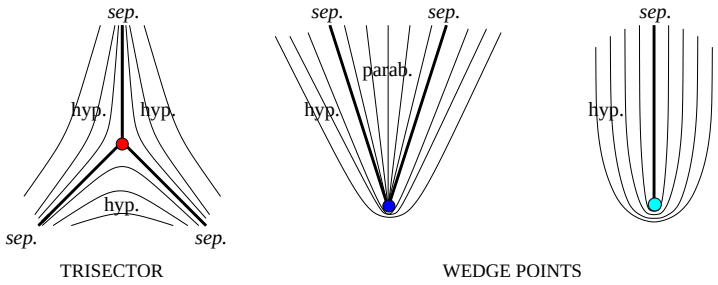

Fig. 1. First Order Degenerate Points

every non-zero vector is an eigenvector in this case. At a degenerate point, the deviator value is a zero matrix. In linear tensor fields, these singularities exist in two possible types: *Trisector* or *wedge point* (see Fig. 1). Due to orientation indeterminacy of tensor lines, these singularities exhibit structures that would be impossible in the oriented, vector case (consider for example the flow on each side of the single line converging toward the singularity in the second type of wedge points). Remark that more general singularities can be encountered in the piecewise linear case as already mentioned in [11].

In the neighborhood of a degenerate point, the regions where tensor lines pass the singularity by in both directions are called hyperbolic. The regions where they reach the singularity, on the contrary, are called parabolic. The curves that converge toward a degenerate point and bound a hyperbolic region are called separatrices. These special tensor lines constitute the edges of the topological graph. According to this definition, a trisector has three hyperbolic sectors and three associated separatrices while a wedge point has one hyperbolic sector and either one or two separatrices. In the latter case the separatrices bound a parabolic sector. Refer to Fig. 1.

2.2 Tensor Index

A major notion for the structural classification of an tensor field is the so-called tensor index. It is computed along a closed non self-intersecting curve as the number of rotations of the eigenvectors when traveling once along the curve in counterclockwise direction. An illustration is shown in Fig. 2. This extends to tensor fields the essential notion of Poincaré index defined for vector fields. Because of the lack of orientation of eigenvectors, the tensor index is a multiple of $\frac{1}{2}$. The index of a region that contains no degenerate point is zero. If the considered region contains a first-order degenerate point we get an index $-\frac{1}{2}$ for a trisector point while a wedge point has index $+\frac{1}{2}$. The index of a region containing several degenerate points is the sum of their individual indices. Remark that in the linear case, since only trisectors and wedges can be encountered, if the index of a closed curve is zero then the enclosed region contains no degenerate point. This property will prove essential in the following.

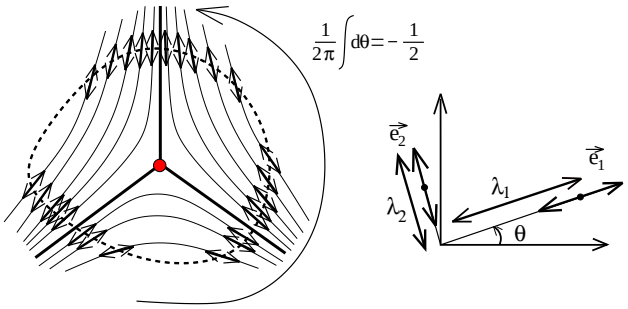

Fig. 2. Tensor index

2.3 Bifurcations

The definitions introduced previously apply to an instantaneous topological state of a tensor field. Now, this stable state may evolve into another one by slight changes of underlying parameters. A typical example is provided by time-dependent tensor fields, the degenerate points of which may move, appear or vanish over time, leading to topological changes. These changes preserve structural consistency and the tensor index acts as a topological invariant. If a topological transition only affects a small region of the field, it is called a *local bifurcation*. If, on the contrary, it leads to a global structural change, it is called a *global bifurcation*. For our purpose we only need to consider a particular kind of local bifurcation: It consists of the pairwise annihilation of a wedge and a trisector point. Since these singularities have global index 0, they are equivalent to a configuration without degenerate point and therefore disappear right after merging. This transition is illustrated in Fig. 3. Additional information on the topic of tensor bifurcations can be found in [13].

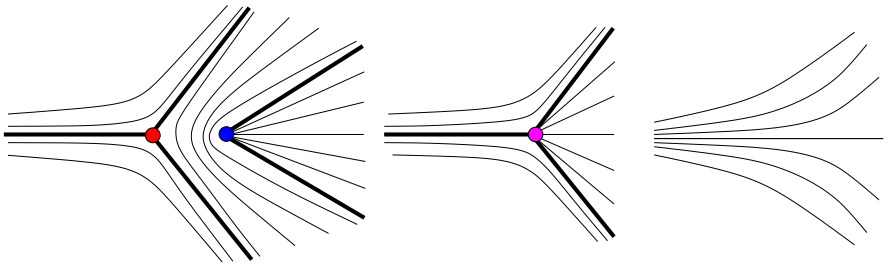

Fig. 3. Pairwise annihilation

Practically, since we want to reduce the number of degenerate points and associated separatrices while being consistent with the original topology, we locally force

pairwise annihilations of a wedge and a trisector. This can be done by small local changes in the field values as we show in the following.

3 Linear Tensor Fields

For the simplification method to come, we first need to consider an important property of linear tensor fields from the topological viewpoint.
As discussed previously, we consider deviator tensor fields written in the form of equation 1, where α and β are linear functions of the position (x, y). The eigenvector $\mathbf{e}_\theta = (\cos\theta, \sin\theta)$ identified by its angular coordinate θ satisfies the relation

$$T\mathbf{e}_\theta \times \mathbf{e}_\theta = 0,$$

where $\times$ stands for cross-product. This leads after calculus to

$$\alpha \sin 2\theta - \beta \cos 2\theta = 0,$$

that is

$$\tan 2\theta = \frac{\beta}{\alpha}.$$

Thus, we get the following differential equation

$$d\theta = \frac{1}{2} \frac{\alpha d\beta - \beta d\alpha}{\alpha^2 + \beta^2}. \tag{2}$$

If we now consider an arbitrary linear interpolated edge $[AB]$ with parametrization $t \in [0, 1]$, we can consider the restriction of T to this edge. We write $\alpha(t) = \alpha_0 + t\alpha_1$ and $\beta(t) = \beta_0 + t\beta_1$. We now compute the angle variation of an eigenvector along $[AB]$ by integrating Equation 2 (remark that this angle variation is the same for both eigenvectors since they are everywhere orthogonal to another):

$$\int_A^B d\theta = \frac{\alpha_0\beta_1 - \alpha_1\beta_0}{2} \int_0^1 \frac{dt}{at^2 + bt + c}$$

where a, b and c are functions of $\alpha_{0,1}$ and $\beta_{0,1}$. Furthermore, the discriminant $\Delta = b^2 - 4ac$ is negative. Therefore it follows (after calculus)

$$\int_A^B d\theta = \frac{\mathrm{sign}(\alpha_0\beta_1 - \alpha_1\beta_0)}{2} (\mathrm{atan}\mu_1 - \mathrm{atan}\mu_0)$$

where μ_0 and μ_1 are two real scalars that depend on $\alpha_{0,1}$ and $\beta_{0,1}$. Since the function atan maps $\mathbb{R}$ onto the open set $(-\frac{\pi}{2}, \frac{\pi}{2})$, we finally obtain

$$\left| \int_A^B d\theta \right| < \frac{\pi}{2}. \tag{3}$$

Thus *the angle variation of an eigenvector along a linear interpolated edge is always smaller than* $\frac{\pi}{2}$.

We use this property now to compute the index of a linear tensor field along the edges of a triangle. Since the field is linear, it is determined by the three tensor values at the vertices of the triangle. We denote by θ_0, θ_1, θ_2 the corresponding angle coordinates of one of both eigenvector fields at these positions, enumerated in counterclockwise order. Because eigenvectors have neither norm nor orientation these angle values are defined modulo π (denoted $[\pi]$ in the following). We set by convention $\theta_3 := \theta_0$, so we have

$$\text{index} = \Sigma_{i=0}^{3} \Delta(\theta_i, \theta_{i+1}). \tag{4}$$

By Equation 3 and using the notation $\delta_i = \theta_{i+1}[\pi] - \theta_i[\pi]$, it comes

$$\Delta(\theta_i, \theta_{i+1}) = \begin{array}{lll} \delta_i & \text{if} & |\delta_i| < \frac{\pi}{2} \\ \delta_i + \pi & \text{if} & \delta_i < -\frac{\pi}{2} \\ \delta_i - \pi & \text{if} & \delta_i > \frac{\pi}{2}. \end{array}$$

4 Selective Pairing of Degenerate Points

As mentioned before, we aim at annihilating pairs of degenerate points of opposite indices. Moreover, the corresponding topology simplification must take geometric and any additional criteria into account to fit the considered interpretation of the tensor field. Our geometric criterion is the proximity of the singularities to be removed pairwise. This choice is motivated by two major reasons. First, close singularities result in small features that clutter the global topology depiction since they can hardly be differentiated and induce many separatrices. Second, piecewise linear interpolation is likely to produce topological artifacts consisting of numerous close first-order singularities, especially if numerical noise is an issue. Therefore, based on a proximity threshold, we determine all possible pairs of wedges and trisectors satisfying the geometric criterion and sort them in increasing distance. Additional criteria may be provided to restrict the range of the considered singularities to those that are little relevant for interpretation. Practically, a quantity is provided that characterizes the relevance of each degenerate point and one retains for simplification only those with a value under a user-prescribed threshold. Thus, if a given singularity is considered important for interpretation, it will be included in no pair and therefore will not be removed from the topology. Remark that compared to the pairing strategy used in previous work for the vector case [12], the connection of both singularities in a pair through a separatrix is not used as criterion. This is because every degenerate point exhibits at least one hyperbolic region which entails that separatrices emanating from a singularity often do not reach any other one.

5 Local Topology Simplification

Once a pair of degenerate points has been identified that fulfills our criteria, it must be removed. To do this, we start a local deformation of the tensor field in a small area around the considered singular points. Practically, we only modify tensor values at the vertices of the triangulation and do not modify the interpolation scheme which obviously ensures continuity over the grid after modification. In the following, we detail first how vertices to be modified are determined and then how new values are set at those vertices to ensure the absence of remaining singularities in their incident cells after processing.

5.1 Cell-wise Connection

The method used here is the same as the one in [12] since the task is the same as in the vector case: Determine well-shaped cell groups that link two singularities over the grid. Consider the situation shown in Fig. 4. We first compute the intersections of the straight line connecting the first degenerate point to the second with the edges of the triangulation. For each intersection point, we insert the grid vertex closest to the second degenerate point (see vertices surrounded by a circle) in a temporary list. After this, we compute the bounding box of all vertices in the list and include all grid vertices contained in this box. Thus, every vertex marked in the former step is included. The use of a bounding box is intended to ensure a well shaped

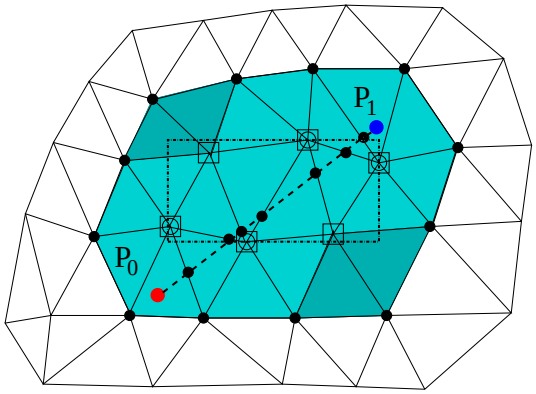

Fig. 4. Cell-wise connection

deformation domain, especially useful if many cells separate both singular points. This configuration occurs if the distance threshold has been assigned a large value to obtain a high simplification rate. The vertices concerned with modification are called *internal vertices* and are shown surrounded by squares. Since the modification of a vertex tensor value has an incidence on the indices of all triangle cells it belongs

to, we include every cell incident to one of the selected vertices in a cell group. These cells are colored in gray. Further processing will have to associate the internal vertices with tensor values that ensure the absence of any singular point in the cell group with respect to the tensor values defined at the *boundary vertices* (marked by black dots in Fig. 4) that will not be changed. The connection may fail if one of the included cells contains a degenerate point that does not belong to the current pair: In this case, the global index of the cell group is no longer zero. If it occurs, we interrupt the processing of this pair. Nevertheless, such cases can be mostly avoided since we simplify pairs of increasing distance.

5.2 Angular Constraints

The basic principle of our simplification technique can be better understood when considering a single internal vertex together with its incident triangles, see Fig. 5. Suppose that every position marked black is associated with a constant tensor value and that the global index of the triangle stencil is zero. The problem consists in determining a new tensor value at the internal vertex (marked white) such that no incident cell contains a degenerate point. This is equivalent to a situation where every incident triangle has index 0 according to what preceedes.

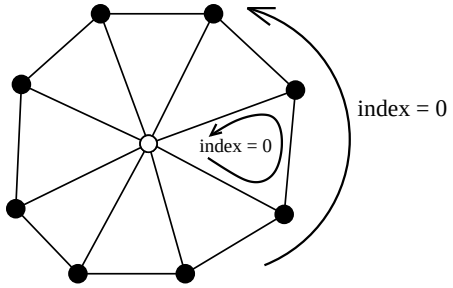

Fig. 5. Configuration with single internal vertex and incident cells

Now, in each triangle the angle coordinates of the eigenvectors defined at the black vertices (say θ_0 and θ_1) induce an angular constraint for the new eigenvector: in equation 3, $\Delta(\theta_0, \theta_1)$ is already set to a value that is strictly smaller than $\frac{\pi}{2}$. The two missing terms must induce a global angle change strictly smaller than π (for the index of a linear degenerate point is a multiple of $\frac{1}{2}$). This condition holds if and only if the new eigenvector value has angle coordinate in $(\theta_1 + \frac{\pi}{2}, \theta_0 + \frac{\pi}{2})$ (modulo π), with $[\theta_0, \theta_1]$ being an interval with width smaller than $\frac{\pi}{2}$, i.e. the actual angle change along a linear edge from θ_0 to θ_1 (see Fig. 6).

This provides a constraint on the new value for a single triangle. Intersecting the intervals imposed by all incident triangles, one is eventually able to determine an interval that fulfills all the constraints. Note that this interval may be empty. In

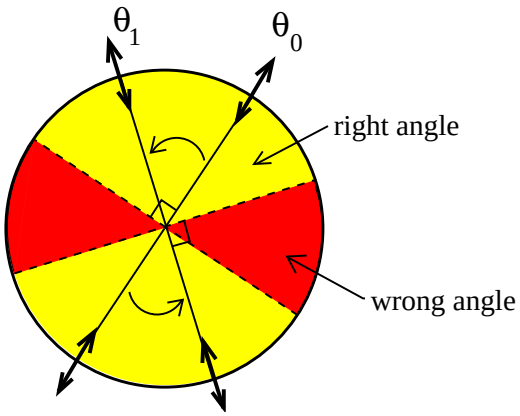

Fig. 6. Angular constraint in a triangle cell

this case, the simplification is (at least temporarily) impossible. Once a satisfactory angle interval has been found for the new eigenvector, we must provide the vertex with a corresponding tensor value. If θ is an angle in the interval then the following tensor value will be solution:

$$T_{new} = \begin{pmatrix} \cos 2\theta & \sin 2\theta \\ \sin 2\theta & -\cos 2\theta \end{pmatrix}.$$

5.3 Iterative Solution

For each internal vertex (see Fig. 4) we must now find a new tensor value that fulfills all the angle constraints induced by the edges connecting the incident vertices. These incident vertices are of two types: internal or boundary vertices. Edges linking boundary vertices are considered constant and induce fixed angular constraints. Internal vertices still must be provided a final tensor value and introduce flexibility in the simplification scheme. Practically, the problem to solve can be seen as an optimization problem. The quantity to minimize for each internal vertex is the distance of its current angle value to the interval of admissible angles induced by its neighbors. This distance is considered zero if the angle lies within the interval. Initially, the angle values of the internal vertices are undefined. During a first iteration, boundary vertices create angular constraints on the adjacent internal vertices. These constraints are then propagated iteratively to their neighbors in the next steps. If the current angle values of the surrounding vertices correspond to an empty interval, their mean value is used as predictor for the next iteration. Consequently, the whole processing can be interpreted as a local constrained smoothing of the tensor field.

The pseudo-code is as follows.

// initialization

```
for each (internal vertex)
   interval = fixed constraints
   if (interval is empty)
      exit
   end if
   if (no fixed constraints)
      interval = [0, PI[
   end if
end for each

// iterations
nb_iterations = 0
repeat
   succeeded = true
   nb_iterations++
   for each internal vertex
      compute mean_angle of processed incident vertices
      if (interval not empty)
         if (mean_angle in interval)
            current_angle = mean_angle
         else
            current_angle =
               best approximation of mean_angle in interval
         end if
      else
         succeeded = false
         if (mean_angle in fixed
             constraints)
            current_angle = mean_angle
         else
            current_angle =
               best approximation of mean_angle in interval
      end if
   end for each
until (succeeded or
       nb_iterations > MAX_NB_ITERATIONS)
```

If one of the internal vertices has incompatible fixed constraints, our scheme will fail. Therefore, we interrupt the process during initialization and move to the next pair. If the iterative process failed at determining compatible angular constraints for all internal vertices, we maintain the current pair and move to the next as well.

6 Results

The dataset used to test our method stems from a CFD simulation. This is the symmetric part of the rate of deformation (i.e. first-order derivative) tensor field of a vortex breakdown simulation that was provided by Wolfgang Kollmann from UC

Davis. Vortex breakdown is a phenomenon observed in a variety of flows ranging from tornadoes to wing tip vortices, pipe flows, and swirling jets. The latter flows are important to combustion applications where they are able to create recirculation zones with sufficient residence time for the reactions to approach completion. This is a typical case of turbulent global structural behavior. The topology exhibits 67 singularities and 140 separatrices as shown in Fig. 7. The rectilinear grid has 123 x 100 cells. Each rectangular cell is split to result in a triangulation containing about 25000 cells. To simplify this topology we only consider the euclidean distance be-

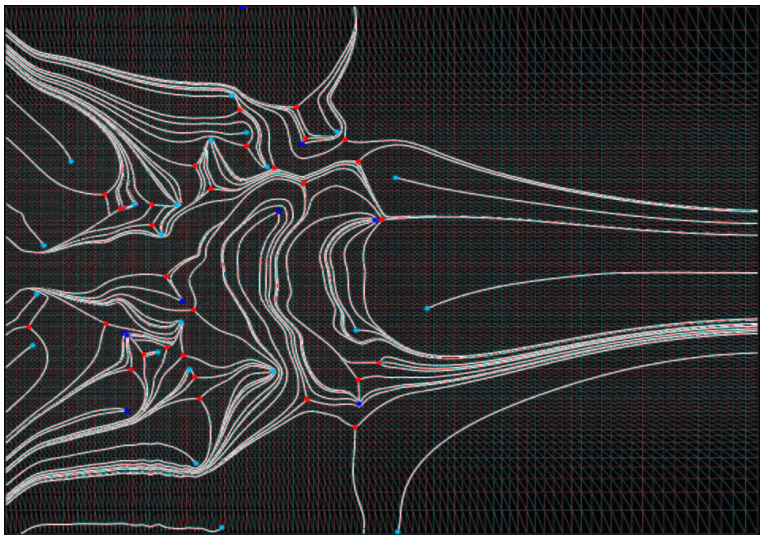

Fig. 7. Initial topology with grid

tween degenerate points as a criterion. Remember however that the method does not impose any restriction on the choice of additional qualitative or quantitative criteria characterizing the importance of a singularity or of a given region of the graph. The first simplified topology is obtained with a tiny distance threshold corresponding to 0.2% of the grid diagonal. Every pair consisting of degeneracies that could not be graphically differentiated has disappeared. There are 59 remaining singularities. The modified areas are indicated by rectangular boxes. See Fig. 8.

Increasing the threshold up to a value of 2% of the grid diagonal, one obtains a topology with 35 remaining singularities as shown in Fig. 9. A noticeably clarified graph can be obtained in this case while global strutural properties of tensor field have been preserved. The highest simplification rate is obtained with a threshold of 5% of the grid diagonal. The corresponding topology is shown in Fig. 10. The fact that this topology cannot be simplified further (even with a very large geometrical threshold) is explained by the presence of incompatible fixed angle constraints on the boundaries of the cell pads containing the remaining pairs. The local deforma-

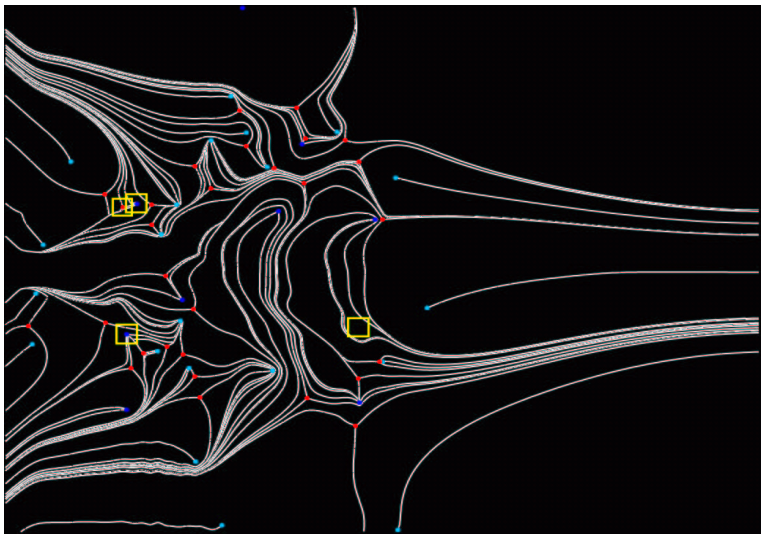

Fig. 8. Simplified topology: distance threshold = 0.2%

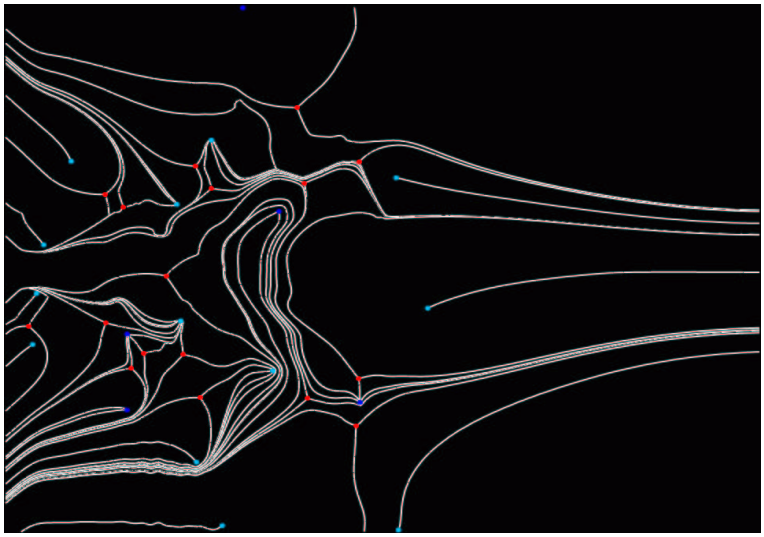

Fig. 9. Simplified topology: distance threshold = 2%

tion corresponding to the simplified topologies shown so far is illustrated in Fig. 11. The topology is displayed together with the underlying cell structure and the eigenvectors.

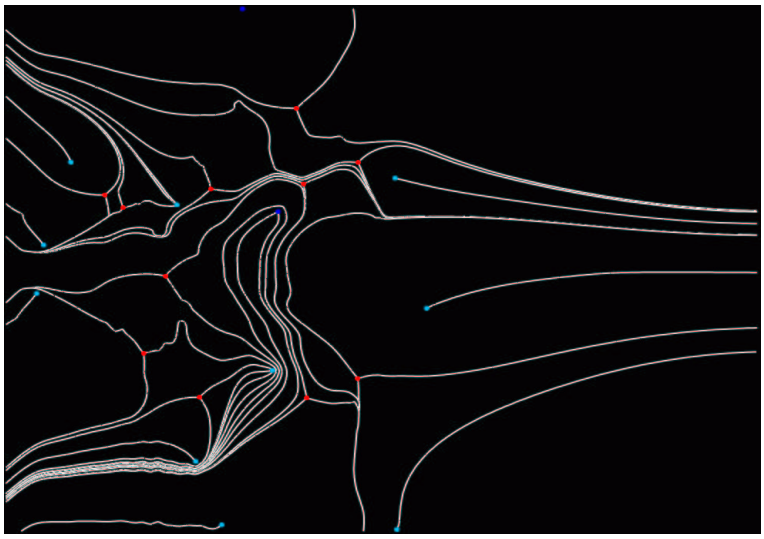

Fig. 10. Simplified topology: distance threshold = 5%

7 Conclusion

We have presented a method that simplifies the topology of turbulent planar, symmetric, second-order tensor fields while preserving structural consistency with the original data. The simplification is achieved by means of successive local deformations of the field that entail the pruning of pairs of degenerate points of opposite indices. The pairing strategy can take geometrical as well as any additional criteria into account to fit the domain of application. The theoretical background of this technique is provided by the notion of bifurcation since the disappearance of a pair of singularities corresponds to the pairwise annihilation of a wedge point and a trisector. The method has been tested on a CFD simulation of a vortex breakdown because this kind of datasets exhibit many complex features that clutter the global depiction. The results demonstrate the ability of the method to remove structural features of small scale while letting the rest of the topology unchanged. This clarifies noticeably the depiction and eases interpretation.

Acknowledgment

The authors wish to thank Wolfgang Kollmann, MAE Department of UC Davis, for providing the vortex breakdown tensor dataset. Furthermore, we would like to thank Tom Bobach, David Gruys, Max Langbein and Martin Öhler for their programming efforts.

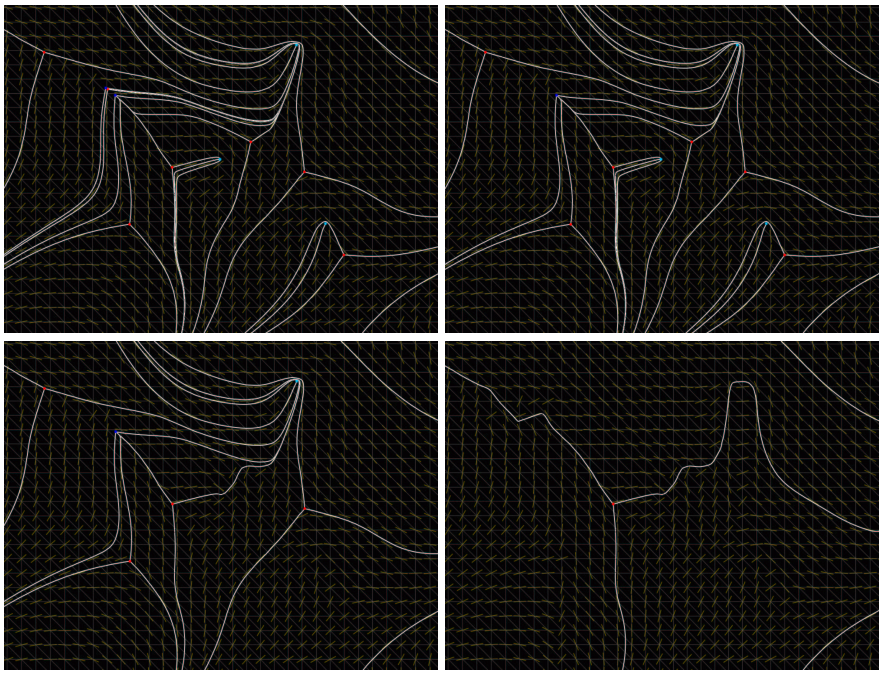

Fig. 11. Local topology simplification: initial graph and simplifications with 0.2%, 2% and 5% as thresholds

References

1. Andronov, A. A., Leontovich, E. A., Gordon, I. I., Maier, A. G., *Qualitative Theory of Second-Order Dynamic Systems*. Israel Program for Scientific Translations, Jerusalem, 1973.
2. Delmarcelle, T., Hesselink, L., *The Topology of Symmetric, Second-Order Tensor Fields*. IEEE Visualization '94 Proceedings, IEEE Computer Society Press, Los Alamitos, 1994, pp. 140-147.
3. Delmarcelle, T., *The Visualization of Second-Order Tensor Fields*. PhD Thesis, Stanford University, 1994.
4. Guckenheimer, J., Holmes, P., *Nonlinear Oscillations, Dynamical Systems and Linear Algebra*. Springer, New York, 1983.
5. Heckel, B., Weber, G., Hamann, B., Joy, K. I., *Construction of Vector Field Hierarchies*. IEEE Visualization '99 Proceedings, IEEE Computer Society Press,
6. Helman, J. L., Hesselink, L., *Visualizing Vector Field Topology in Fluid Flows*. IEEE Computer Graphics and Applications, 1991. pp.36-46. Los Alimitos, 1999, pp. 19-25.
7. W. de Leeuw, R. van Liere, *Collapsing Flow Topology Using Area Metrics*. IEEE Visualization '99 Proceedings, IEEE Computer Society Press, Los Alamitos, 1999, pp. 349-354.

8. Nielson, G. M., Jung, I.-H., Sung, J., *Wavelets over Curvilinear Grids*. IEEE Visualization '98 Proceedings, IEEE Computer Society Press, Los Alamitos, 1998, pp. 313-317.
9. Spivak, M., *A Comprehensive Introduction to Differential Geometry, Vol. 1-5* Publish or Perish Inc., Berkeley CA, 1979.
10. Tricoche, X., Scheuermann, G., Hagen, H., *A Simplification Method for 2D Vector Fields*. IEEE Visualization '00 Proceedings, IEEE Computer Society Press, Los Alamitos, 2000, pp. 359-366.
11. Tricoche, X., Scheuermann, G., Hagen, H., *Vector and Tensor Field Topology Simplification on Irregular Grids*. Proceedings of the Joint Eurographics-IEEE TCVG Symposium on Visualization in Ascona, Switzerland, D. Ebert, J. M. Favre, R. Peikert (eds.), Springer-Verlag, Wien, 2001, pp. 107-116.
12. Tricoche, X., Scheuermann, G., Hagen, H., *Continuous Topology Simplification of 2D Vector Fields*. IEEE Visualization '01 Proceedings, IEEE Computer Society Press, Los Alamitos, 2001.
13. Tricoche, X., *Vector and Tensor Topology Simplification, Tracking, and Visualization*. PhD thesis, Schriftenreihe / Fachbereich Informatik, Universität Kaiserslautern, 3, 2002.